AALBORG UNIVERSITY
DENMARK

A Novel Dynamic Aggregation Modeling Method of Grid-Connected Inverters

Application in Small-Signal Analysis

Liao, Shuhan; Zha, Xiaoming; Li, Xianzhe; Huang, Meng; Sun, Jianjun; Pan, Jing; Guerrero, Josep M.

Publication date:
2019

Document Version
Accepted author manuscript, peer reviewed version

Link to publication from Aalborg University

A Novel Dynamic Aggregation Modeling Method of Grid-Connected Inverters: Application in Small-Signal Analysis

Shuhan Liao, *Student Member, IEEE*, Xiaoming Zha, *Member, IEEE*, Xianzhe Li, Meng Huang, *Member, IEEE*, Jianjun Sun, *Member, IEEE*, Jing Pan, Josep M. Guerrero, *Fellow, IEEE*

Abstract—Converter-control-based generators (CCBGs) exhibit different dynamic characteristics compared with traditional synchronous generators, and thus affect the oscillation modes and small-signal stability of power systems in a different manner. Simplified representation of a great number of grid-connected inverters is indispensable for efficient and accurate dynamic analysis of power systems integrated with large-scale renewable energy generation. This paper proposes a novel dynamic aggregation modeling method of grid-connected inverters using coherency-based equivalence, and validates the applicability of the aggregated model for small-signal stability analysis. Modal analysis and dynamic simulation are conducted on the detailed model and aggregated models of the test system. The frequency-domain results and the time-domain results from PSCAD/EMTDC both verify the adequacy of the coherent equivalence practice in the small-signal rotor angle stability analysis.

Index Terms—Dynamic aggregation, inverter, small-signal stability, renewable energy, coherency-based equivalence.

I. INTRODUCTION

THE increasing penetration of converter-control-based generators (CCBGs), like permanent magnetic synchronous generators (PMSGs) and photovoltaic (PV) generators, has been reported to have positive or negative effects on the small-signal stability of power systems [1-3]. There are two types of mechanism which can explain the impact of the CCBGs integration on electromechanical oscillatory modes (EOMs) and small-signal rotor angle stability of power systems: 1) impacting the power flow of power systems; 2) converter control in CCBGs interacting with the dynamic of synchronous generators (SGs) [4-6]. The schematic of a typical CCBG, a PMSG-based wind turbine generator (WTG) and its influence
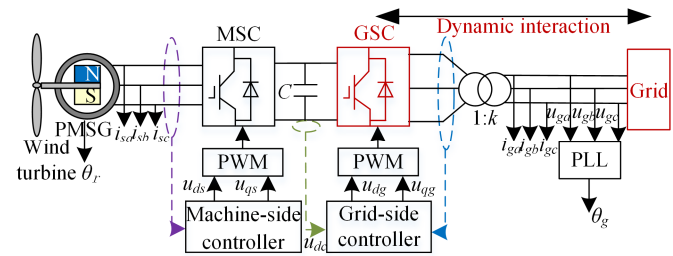
Fig. 1. The schematic of grid-connected PMSG-based WTG.

mechanism on small-signal stability is indicated in Fig. 1.

These two mechanisms can be analyzed in a decoupled way [5]. When the small-signal issues introduced by the change of power flow are concerned, the entire CCBG can be simply modeled by a power source to exclude the impact of dynamic interactions [5-7]. When the dynamic interaction is studied, the structure and control of grid-side converter (GSC) should be modeled in detail and the mechanical parts are regarded as invariant input power to exclude the impact of power flow variations [4], [5], [8]. Therefore, the accurate representation of probabilistic characteristics of the output of CCBGs is adequate for studying the impact of CCBGs on the small-signal stability of power systems driven by mechanism 1), while the accurate dynamic model of CCBGs is indispensable for research on the dynamic interaction between CCBGs and SGs. Whatever mechanism is concerned, modal analysis based on the linearized model is a widely-used method for the analysis of EOMs and small-signal stability of CCBGs-integrated power systems.

Modal analysis based on the detailed model of a CCBG plant represented by every individual CCBG is time-consuming, considering the great number of CCBGs in a plant and the complexity of the CCBG itself. To explore the influence mechanism of CCBGs in a convenient way, many studies exploit a WTG and a PV generator to represent a wind farm (WF) and a PV station, respectively [9-11]. In practical applications, this single-machine model will cover up some details in terms of the dynamic characteristics of a whole CCBG station. Thus, multimachine representation, which aggregates CCBGs with similar dynamic characteristics based on a specific grouping criterion, is proposed to mitigate this problem [12].

Previous coherency-based equivalence methods of CCBGs normally focus on the accuracy of the long time-scale transient's equivalence. Taking the aggregation of WTGs as an ex-

ample, they are normally grouped based on the wind direction, wind speed [13], and layout of wind farms [14]. Besides, clustering algorithms are used to represent the probabilistic characteristics of a WF [15]. Aggregated models based on these criteria yield a good performance in simulating the power change of a detailed model due to wind fluctuation, and thus can evaluate the influence of the change of power flow on the small-signal stability efficiently and accurately. However, aggregated models which group WTGs with similar wind speeds cannot guarantee the accuracy in the dynamic characteristics of inverters. Exploiting these aggregated models may fail to draw correct conclusions for the analysis of the dynamic interaction between CCBGs and SGs, because the dynamic interaction is directly affected by control parameters and dynamic characteristics of inverters [4]. Therefore, the aggregation modeling capable of fitting the dynamic characteristics of the detailed model of inverters is a key issue for its application in the small-signal analysis.

As for the aggregation of inverters, a structure-preserving model is proposed in [16] and [17], and the dynamical states of this aggregated model are the same as those of every individual inverter. However, inverters of concern in [16] and [17] have identical parameters, so that the coherency identification is still not considered. To the best of our knowledge, only [18] and [19] have presented the coherency-based equivalence method for inverters. In [18], the principle of coherency in differential geometry is applied to the coherency identification of inverters, but the coherency criterion is hard to be measured and the effect of equivalence has not been verified. The authors of [19] presented a coherent equivalence method for modular multilevel converters (MMCs) with virtual synchronous generator (VSG) control. In [19], virtual power angles (VPAs) are used to identify the coherency for VSG-based MMCs, considering the similarity in dynamic behaviors of SGs and VSG-controlled MMCs. This equivalent model can simulate the dynamic performance of paralleled VSG-controlled inverters well, but cannot be developed for inverters controlled by other strategies. Therefore, a universal coherency criterion of inverters is still so far unexplored in the literature, and there is lack of an appropriate dynamic aggregation modeling method of GSCs for efficient dynamic interaction analysis. This paper is trying to fill this gap by applying Hamilton's action to the deduction of the coherency criterion for grid-connected inverters from the perspective of energy. The reason is that Hamilton's action has the exclusive feature to represent the comprehensive dynamic characteristics of dynamical systems, including electric systems [20].

This paper proposes a novel dynamic aggregation method for inverters and validates the applicability of the aggregated model in small-signal analysis of CCBGs-integrated power systems. In section II, the coherency criterion of inverters is deduced based on Hamilton's action, and the calculation method of equivalent parameters is presented. Section III introduces the linearized model of CCBGs-integrated power systems and the analysis method of dynamic interactions. In section IV, an example is presented to demonstrate the application of the proposed aggregation modeling method in
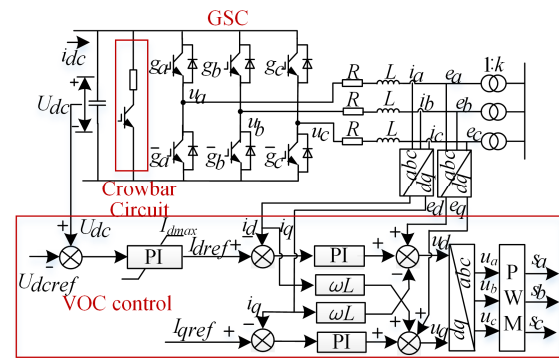

Fig. 2. The structure and control scheme of grid-connected inverters.

small-signal stability analysis. Time-domain simulation is conducted by using the PSCAD/EMTDC software.

II. COHERENCY-BASED EQUIVALENCE METHOD

In the small-signal analysis, a dynamic aggregation model of inverters is indispensable for efficient analysis of dynamic interactions between CCBGs and SGs. The structure and control scheme of inverters in this paper is shown in Fig. 2. The inverters are controlled by voltage orientation control (VOC) in normal states. There is saturation in the PI of the dc voltage loop, and crowbar circuit comes into operation under faults.

This section proposes a novel coherent equivalence method to aggregate inverters for dynamic interaction analysis. The aggregated model preserves the original structure of an individual inverter. The steps of the method are coherency identification and parameters aggregation.

A. Coherency Identification

The key issue of the coherent equivalence method applied to inverters is to find the coherency criterion, which can identify inverters with similar dynamic characteristics. Hamiltonian mechanics is applied to inverters to deduce coherency criterion, because the Hamilton principle is equivalent to the state equation of a dynamic system and can represent the comprehensive dynamic characteristics of a system [21]. With energy exchange in dc and ac sides, a grid-connected inverter is a nonconservative dynamical system. The Hamilton principle of nonconservative systems is [20]:

$$\delta S = -\int_0^\tau \sum Q_j \delta q_j dt \quad (j=1,2,\cdots,N) \qquad (1)$$

where S is Hamilton's action, q_j is generalized coordinates, Q_j is nonconservative forces projected to corresponding coordinates, and N is the number of generalized coordinates. For electric systems, Q_j is the voltage which can produce the power flow between the energy storage elements and the external system.

The explicit expression of S is [20]:

$$S = \int L_a dt = \int (T-V)dt \qquad (2)$$

where L_a is the Lagrangian function, T is magnetic field energy, and V is electric field energy.

Seen from (1), S and Q_j codetermine the variation of state variables of inverters. To deduce the coherency criterion of inverters, a new physical quantity is needed to independently represent the comprehensive dynamic characteristics of non-

conservative systems. To meet this demand, the generalized Hamilton's action $\hat{S}$ is defined as:

$$\hat{S} = \int \hat{L}_a dt = \int (T - V - U) dt \tag{3}$$

where U represents the energy $-\sum_{j=1}^{N} \int_{\gamma} Q_j dq_j$.

Based on (3), the Hamilton's principle shown in (1) can be rewritten as:

$$\delta \hat{S} = 0 . \tag{4}$$

The proof of the equivalence between (1) and (4) is presented in the Appendix A. In this way, (4) is also equivalent to state equations of a dynamical system. It is clear that the Hamilton's principle expressed by (4) is only related with $\hat{S}$. That is to say, $\hat{S}$ can independently represent the whole dynamic characteristics of nonconservative systems, and thus can be used for the deduction of the coherency criterion for inverters.

For inverters shown in Fig. 2, T is the magnetic field energy on the inductor, V is the electric filed energy on the capacitor:

$$\begin{cases} T = L(\dot{q}_{La}^2 + \dot{q}_{Lb}^2 + \dot{q}_{Lc}^2)/2 \\ V = CU_{dc}^2/2 = q_C^2/2C \end{cases}, \tag{5}$$

where the meaning of L, C, R, and U_{dc} are shown in Fig. 2, q_C is the electric charge of capacitor C, and q_{Lk} is the electric charges on the filter inductor L of three phases.

The Q_j in inverters refers to the grid voltage, the voltage across the resistor R, and the dc power supply voltage which equals to voltage across dc capacitor, so that $\sum_{j=1}^{N} \int_{\gamma} Q_j dq_j$ is the sum of energy output in the ac side, energy dissipation on the resistor and the energy input in the dc side:

$$\sum_{j=1}^{N} \int_{\gamma} Q_j dq_j = -\int \sum_{k=a,b,c} e_k \dot{q}_{Lk} dt - \int (R \sum_{k=a,b,c} \dot{q}_{Lk}^2) dt + \int U_{dc}(\dot{q}_C + \sum_{k=a,b,c} s_k \dot{q}_{Lk}) dt \tag{6}$$

where e_k is the grid voltage, and s_k is bipolar switching function.

Substitute (5) and (6) into (3):

$$d\hat{S} = \hat{L}_a dt = [(L \sum_{k=a,b,c} \dot{q}_{Lk}^2)/2 - q_C^2/2C - \int (R \sum_{k=a,b,c} \dot{q}_{Lk}^2) dt + \int U_{dc}(\dot{q}_C + \sum_{k=a,b,c} s_k \dot{q}_{Lk}) dt - \int \sum_{k=a,b,c} e_k \dot{q}_{Lk} dt] dt \tag{7}$$

Strictly, if all the state variables of an inverter are proportional respectively to the state variables of another inverter, these two inverters are coherent. Based (7), this criterion can be proven to be equivalent to:

$$\Delta \hat{S}_1(t)/\Delta \hat{S}_2(t) = K \tag{8}$$

where the subscripts are numbers of inverters; $t \in [t_0, t_0 + \tau]$, t_0 is the time when the disturbance is imposed; τ is the duration of coherency identification and set as 0.2-0.5 s for inverters based on dynamic response time; $\Delta \hat{S} = \hat{S}(t) - \hat{S}(t_0)$; K is a constant.

Because $\hat{S}$ is a universal expression for inverters controlled by any strategy, the coherency criterion based on $\hat{S}$ is a universal coherency criterion of inverters. Considering that $\hat{S}(t)$ is the time integral of $\hat{L}_a(t)$, (8) can be rewritten as:

$$L_{a1}/L_{a2} = (T_1 - V_1 - U_1)/(T_2 - V_2 - U_2) = K \tag{9}$$

From energy conservation law, we have $T_1 + V_1 + U_1 = E_1$ and $T_2 + V_2 + U_2 = E_2$, where E_1 and E_2 are the total energy of inverter 1

and inverter 2, respectively. By substituting the equations of energy conservation law into (9), we can obtain:

$$T_1/T_2 = K \tag{10}$$

According to the definition of the magnetic field energy stored in inductors, (10) is transformed into:

$$i_{k1}/i_{k2} = \sqrt{KL_2/L_1} = k_i \tag{11}$$

where i_k represents three-phase instantaneous line currents of inverters, and k_i is a constant.

The criterion can be relaxed to some extent for application:

$$\max_{t \in [t_0, t_0 + \tau]} |i_{k1}(t)/i_{k2}(t) - k_i| \le \varepsilon \tag{12}$$

where ε is the specified tolerance of the criterion.

The coherency of inverters can be identified using the criterion shown in (12), and then every coherent inverter group can be aggregated as a single inverter to represent the dynamic characteristics of the whole group.

B. Calculation of Equivalent Parameters

Equivalent circuit and control parameters are needed for aggregated models. The aim of parameter equivalence is to guarantee the high accuracy in output power of a REG plant during a dynamic process.

Inverters of a REG plant is in parallel. To guarantee the accuracy in output power and line currents, the equivalence process of circuit parameters can be seen as the parallel of every single circuit. Thus, equivalent circuit parameters are [19]

$$\begin{cases} L_{eq} = L_1 //L_2 //\ldots //L_n \\ R_{eq} = R_1 //R_2 //\ldots //R_n \\ C_{eq} = C_1 //C_2 //\ldots //C_n \end{cases} \tag{13}$$

where n is the number of coherent inverters, the subscript i and eq represent the serial number of inverters and equivalent parameters, respectively.

The transfer function of the current loop $\varphi(s)$ is [22]

$$\varphi(s) = I_d(s)/I_{dref}(s) = (k_{pi}s + k_{ii})/[Ls^2 + (k_{pi} + R)s + k_{ii}] \tag{14}$$

where k_{pi} and k_{ii} are proportional and integral coefficients of the current loop, respectively.

Ideally, the line currents of an aggregated model should be equal to the sum of line currents of all the inverters in the system. The equivalent transfer function of the current loop $\varphi_{eq}(s)$ can be obtained based on this condition:

$$\varphi_{eq}(s) = \sum_{i=1}^{n} c_i \varphi_i(s)/\sum_{i=1}^{n} c_i \tag{15}$$

where c_i is the capacity of inverter i.

The equivalent proportional and integral coefficients of the current loop are obtained by frequency-domain least square method to fit the dynamic characteristics of (15) [23].

When equivalent PI parameters of the voltage loop is calculated, the dynamic process of current loop can be ignored. In this case, the power balance equation of inverters operating under unity power factor can be written as:

$$CU_{dc}(dU_{dc}/dt) = P_{in} - 1.5e_d(k_{pv} + k_{iv}/s)(U_{dcref} - U_{dc}) \tag{16}$$

where P_{in} is the input power of the dc link, e_d is d-axis voltage on the line side, k_{pv} and k_{iv} are proportional and integral coefficients of the dc voltage loop, respectively.

If two inverters are coherent, dc link voltages of them are equal or proportional to each other. Thus, by adding up all power balance equations of inverters, equivalent proportional and integral coefficients of voltage controller represented by k_{pveq} and k_{iveq} are deduced as

$$\begin{cases} k_{pveq} = \sum_{i=1}^{n} k_{pvi} \\ k_{iveq} = \sum_{i=1}^{n} k_{ivi} \end{cases} \quad (17)$$

where k_{pvi} and k_{ivi} are proportional and integral parameters of voltage loop of inverter i, respectively.

The small-signal characteristics of a synchronous reference frame (SRF) PLL is

$$\Delta\theta = \Delta v_q (k_{pth} + k_{ith}/s)/s \quad (18)$$

where k_{pth} and k_{ith} are proportional and integral parameters, respectively.

The variation of v_q is the same for the aggregated PLL and every single PLL in the detailed model. Thus, the equivalent proportional and integral parameters of PLL, represented by k_{ptheq} and k_{itheq} respectively, are given by weighted mean value of PLLs of the detailed model:

$$\begin{cases} k_{ptheq} = \sum_{i=1}^{n} c_i k_{pthi} / \sum_{i=1}^{n} c_i \\ k_{itheq} = \sum_{i=1}^{n} c_i k_{ithi} / \sum_{i=1}^{n} c_i \end{cases} \quad (19)$$

where k_{pthj} and k_{vthj} are proportional and integral parameters of PLL of inverter i, respectively.

As for the network aggregation, it has been presented in [24] that the size of cable impedance is much smaller than that of the leakage impedance of the transformer, and the aggregation of the network is thus not considered without significant loss in accuracy. The equivalent impedance of transformer Z_{eq} is calculated by:

$$Z_{eq} = Z_1 // Z_2 // \cdots // Z_n \quad (20)$$

where $Z_i (1, 2, \cdots, n)$ is the impedance of the individual transformer, and n is the number of inverters aggregated.

C. Procedure of the Aggregation Modeling

Although the expression of generalized Hamilton's action is complex, the application of the Hamilton's-action-based coherent equivalence method is quite simple. The steps of the proposed method are summarized as follows.

① Obtaining line currents of inverters during a disturbance.

② Calculating $\max\limits_{t \in [t_0, t_0+\tau]} |i_{k1}(t)/i_{k2}(t) - k_i|$ between every two inverters and identifying coherency based on (12).

② Calculating equivalent parameters of the aggregated model based on (13), (15), (17), and (19).

It is noticeable that in step ①, the currents are obtained under the three-phase fault with a 100% voltage sag. This is the severest disturbance that inverters may suffer. Severer fault condition can cause severer dynamic processes of inverters, and it sees more obvious difference of dynamic characteristics among paralleled inverters attributed to different circuit and control parameters. Therefore, the clustering of inverters under three-phase fault with the deepest voltage sag is the most rig-

orous, and the result of coherency under this severe condition is applicable to other disturbances, whether small or large.

Naturally, aggregated models based on this coherency criterion can fit the detailed model well in small- and large-signal cases, and can be applied to small- and large-signal dynamic analyses of CCBGs-integrated systems. In this paper, the impact of CCBGs on the EOMs is concerned, so that the aggregated model needs to be further linearized for the small-signal analysis.

III. APPLICATION OF THE AGGREGATED MODEL IN SMALL-SIGNAL STABILITY ANALYSIS

In this section, the fundamentals of modal analysis are presented at first. Then, the linearized model of multi-CCBGs-integrated power systems is established. Because the dynamic interaction actually exists between GSCs and SGs, as is stated in [4], [5], the dynamic equations of mechanical part and machine-side converter (MSC) are not included in the linearized model. A step-by-step procedure of the coherent equivalence model practice in the small-signal stability analysis is given at the end of this section.

A. Fundamentals of Small-Signal Stability Analysis

The small-signal dynamics of a CCBGs-integrated power system can be represented by the linearized model of the whole system. The linearized model is given by

$$s\Delta\mathbf{X} = \mathbf{J}\Delta\mathbf{X} \quad (21)$$

An m-order system has m states and m real or complex eigenvalues. A pair of complex eigenvalues is a mode of a system. Associations between states and modes can be ascertained by participation matrix $\mathbf{P}$. The kith element of $\mathbf{P}$, represented by p_{ki}, gives the association between the kth-state and the ith-mode:

$$p_{ki} = u_{ki} v_{ki} \quad (22)$$

where u_{ki} is the kith element of the left modal matrix and v_{ki} is the kith element of the right modal matrix.

The sum of participation factors of all state variables associated with the mode i equals to 1 [4]:

$$\sum_{k=1}^{m} p_{ki} = 1 \quad (23)$$

where m is the order of a CCBGs-integrated power system.

Participation factors of EOMs can represent what components of the power system exhibit the EOMs' frequency response, and how these states dynamically interact with each other. Therefore, modal analysis on the basis of linearized modeling is an effective tool to evaluate the dynamic interaction between SGs and CCBGs of a power system.

By analogy with the electromechanical correlation ratio, the grid-side converter participation index (GSC PI) for mode i is defined to evaluate the dynamic interaction quantitively:

$$\text{GSC PI} = \frac{\left| \sum\limits_{k \in gs} p_{ki} \right|}{\left| 1 - \sum\limits_{k \in gs} p_{ki} \right|} \quad \text{for mode } i \quad (24)$$

where gs is the abbreviation of GSC states, and $\sum_{k \in gs} p_{ki}$ is the summation of the participation factors of all GSCs state variables associated with the specific mode i. According to the

feature of participation factors shown in (23), it is obvious that the denominator of (24) is the summation of participation factors of the state variables other than those of the GSC.

If state variables of a GSC are dominant in mode i, GSC PI$\gg$1. Conversely, GSC PI$\ll$1. The value of GSC PI can quantify the comprehensive participation of state variables of a GSC associated with a specified mode i.

Synchronous generator participation index (SG PI) is also defined to evaluate the participation of SGs' states in a mode i:

$$\text{SG PI}=\frac{\left|\sum_{k \in ss} p_{ki}\right|}{\left|1-\sum_{k \in ss} p_{ki}\right|} \quad \text{for mode } i \qquad (25)$$

where the ss is the abbreviation of SG states.

High GSC PI for an EOM indicates a significant impact of CCBGs on rotor angle stability and a strong dynamic interaction between CCBGs and SGs. The SG PI calculated for every SG in a system can further identify which SG is dominant in this EOM and mainly interacts with CCBGs.

B. The Application of Small-Signal Stability Analysis

A SG is modeled by a set of linearized differential equations that represent the dynamic components of the system, and a set of algebraic equations that represent the relationship between currents and fluxes. The linearized model of multiple SGs is

$$\begin{cases} s\Delta \mathbf{X}_{gen} = \mathbf{A}_g \Delta \mathbf{X}_{gen} + \mathbf{B}_{gv}\Delta \mathbf{V}_{g,xy} \\ \Delta \mathbf{I}_{g,dq} = \mathbf{C_g}\Delta \mathbf{X}_{gen} \end{cases} \qquad (26)$$

where $\mathbf{X}_{gen}$ is the state variable vector of SGs, consisting of state variables of mechanical part, electrical part, power system stabilizer (PSS), automatic voltage regulator (AVR), and prime motor. In (26), the subscripts xy indicates the x and y components, dq indicates the d and q components, $\mathbf{V}_g$ is the terminal voltage vector of SGs, and $\mathbf{I}_g$ is the stator currents vector.

For inverters with VOC [25], the linearized model without consideration of PLL dynamic can refer to [8]. In this paper, the dynamic of PLL is added. From (18), it can have:

$$d\Delta \theta_{pll} / dt = \Delta \omega_c \qquad (27)$$

$$d\Delta \omega_c / dt = k_{pth}d\Delta v_q / dt + k_{ith}\Delta v_q \qquad (28)$$

Thus, the linearized model of CCBGs is obtained by integrating (27), (28) with the model given in [8]:

$$s\Delta \mathbf{X}_{con} = \mathbf{A}_v \Delta \mathbf{X}_{con} + \mathbf{B}_{vg}\Delta \mathbf{X}_{gen} + \mathbf{B}_v \Delta v_d \qquad (29)$$

where $\mathbf{X}_{con}$ is the state variables vector of all the CCBGs, consisting of inductor current, capacitor voltage, and other state variables associated with controllers and PLLs. In (29), v_d is the d-axis voltage of the bus with which CCBGs are connected. Every CCBG is represented by an 8th-order model. If n CCBGs are integrated with the system, $\mathbf{X}_{con}$ contains $8n$ state variables.

When the steady-state value of q-axis voltage of the CCBGs-connected bus is 0, Δv_d can be obtained by xy-dq transformation:

$$\Delta v_d = \mathbf{T}_{v1}\Delta \mathbf{V}_{c,xy} \qquad (30)$$

where $\mathbf{T}_{v1}=[\cos\theta_0 \; \sin\theta_0]$, θ_0 is the initial value of PLL output angle, and $\mathbf{V}_c$ is the voltage vector of the CCBG-connected bus.

Substitute (30) into (29):

$$s\Delta \mathbf{X}_{con} = \mathbf{A}_v \Delta \mathbf{X}_{con} + \mathbf{B}_{vg}\Delta \mathbf{X}_{gen} + \mathbf{B}_v \mathbf{T}_{v1}\Delta \mathbf{V}_{c,xy} \qquad (31)$$

The differential equations in (26) and (31), which represent the dynamics of SGs and CCBGs respectively, can be integrated as a whole by using a set of algebraic equations that describe the quasi-static behavior of the transmission network:

$$\begin{bmatrix} \Delta \mathbf{I}_{g,xy} \\ \Delta \mathbf{I}_{c,xy} \\ 0 \end{bmatrix} = \begin{bmatrix} \mathbf{Y}_{gg} & \mathbf{Y}_{gc} & \mathbf{Y}_{gn} \\ \mathbf{Y}_{cg} & \mathbf{Y}_{cc} & \mathbf{Y}_{cn} \\ \mathbf{Y}_{ng} & \mathbf{Y}_{nc} & \mathbf{Y}_{nn} \end{bmatrix} \begin{bmatrix} \Delta \mathbf{V}_{g,xy} \\ \Delta \mathbf{V}_{c,xy} \\ \Delta \mathbf{V}_{n,xy} \end{bmatrix} \qquad (32)$$

where $\mathbf{I}_g$ is the stator currents vector, and $\mathbf{I}_c$ is the output current of the whole CCBG plant. $\mathbf{V}_n$ is the voltage vector, where the elements are the voltage of all nodes, except for those nodes connected with SGs and CCBGs. For power systems integrated with n CCBGs, we have

$$\mathbf{I}_{c,xy} = \Sigma_{i=1}^n \mathbf{I}_{ci,xy} \qquad (33)$$

where $\mathbf{I}_{ci}$ is the output current of the ith CCBG, $\mathbf{I}_{ci,xy}=[I_{ci,x}, I_{ci,y}]^{\mathrm{T}}$.

The $\Delta \mathbf{V}_{g,xy}$ and the $\Delta \mathbf{V}_{c,xy}$ are obtained by three algebraic equations shown in (32), and are simply expressed as:

$$\Delta \mathbf{V}_{g,xy} = \mathbf{R}_{gg}\Delta \mathbf{I}_{g,xy} + \mathbf{R}_{gc}\Delta \mathbf{I}_{c,xy} \qquad (34)$$

$$\Delta \mathbf{V}_{c,xy} = \mathbf{R}_{cg}\Delta \mathbf{I}_{g,xy} + \mathbf{R}_{cc}\Delta \mathbf{I}_{c,xy} \qquad (35)$$

The detailed deduction and expression of matrices $\mathbf{R}_{gg}$, $\mathbf{R}_{gc}$, $\mathbf{R}_{cg}$, $\mathbf{R}_{cc}$ are omitted in this paper.

The xy components $\Delta \mathbf{I}_{g,xy}$ and $\Delta \mathbf{I}_{c,xy}$ can be expressed by dq components using the dq-xy transformation:

$$\Delta \mathbf{I}_{g,xy} = \mathbf{T}_{g0}\Delta \mathbf{I}_{g,dq} + \mathbf{B}_{gI}\Delta \mathbf{X}_{gen} \qquad (36)$$

$$\Delta \mathbf{I}_{c,xy} = \mathbf{T}_{v0}\Sigma_{i=1}^n \Delta \mathbf{I}_{ci,dq} + \Sigma_{i=1}^n \mathbf{B}_{vIi}\Delta \theta_i \qquad (37)$$

The deduction and expression of matrices $\mathbf{T}_{g0}$, $\mathbf{B}_{gI}$, $\mathbf{T}_{v0}$, and $\mathbf{B}_{vIi}$ are presented in Appendix B.

Substitute (34), (36), and (37) into the first equation of (26):

$$s\Delta \mathbf{X}_{gen} = (\mathbf{A}_g + \mathbf{B}_{gv}\mathbf{R}_{gg}\mathbf{B}_{gI} + \mathbf{B}_{gv}\mathbf{R}_{gg}\mathbf{T}_{g0}\mathbf{C_g})\Delta \mathbf{X}_{gen}$$
$$+\mathbf{B}_{gv}\mathbf{R}_{gc}(\mathbf{T}_{v0}\Sigma_{i=1}^n \Delta \mathbf{I}_{ci,dq} + \Sigma_{i=1}^n \mathbf{B}_{vIi}\Delta \theta_i) \qquad (38)$$

As $\mathbf{I}_{ci,dq}$ and θ_i are state variables of CCBGs, (38) is written as:

$$s\Delta \mathbf{X}_{gen} = \mathbf{A}_{gg}\Delta \mathbf{X}_{gen} + \mathbf{A}_{gv}\Delta \mathbf{X}_{con} \qquad (39)$$

Substitute (35), (36), and (37) into (31):

$$s\Delta \mathbf{X}_{con} = \mathbf{A}_v\Delta \mathbf{X}_{con} + \mathbf{B}_v\mathbf{T}_{v1}\mathbf{R}_{cc}(\mathbf{T}_{v0}\Sigma_{i=1}^n \Delta \mathbf{I}_{ci,dq} + \Sigma_{i=1}^n \mathbf{B}_{vIi}\Delta \theta_i)$$
$$+(\mathbf{B}_{vg} + \mathbf{B}_v\mathbf{T}_{v1}\mathbf{R}_{cg}\mathbf{T}_{g0}C_g + \mathbf{B}_v\mathbf{T}_{v1}\mathbf{R}_{cg}\mathbf{B}_{gI})\Delta \mathbf{X}_g$$
$$(40)$$

Similarly, (40) is rewritten as:

$$s\Delta \mathbf{X}_{con} = \mathbf{A}_{vv}\Delta \mathbf{X}_{con} + \mathbf{A}_{vg}\Delta \mathbf{X}_{gen} \qquad (41)$$

By integrating (39) and (41), the linearized model of a power system integrated with n CCBGs is obtained:

$$s\begin{bmatrix} \Delta \mathbf{X}_{gen} \\ \Delta \mathbf{X}_{con} \end{bmatrix} = \begin{bmatrix} \mathbf{A}_{gg} & \mathbf{A}_{gv} \\ \mathbf{A}_{vg} & \mathbf{A}_{vv} \end{bmatrix} \begin{bmatrix} \Delta \mathbf{X}_{gen} \\ \Delta \mathbf{X}_{con} \end{bmatrix} \qquad (42)$$

where nonzero matrices $\mathbf{A}_{gv}$ and $\mathbf{A}_{vg}$ represent dynamic interactions between SGs and CCBGs, as the dynamic characteristics of state variables associated with SGs are affected by state variables of CCBGs and vice versa.
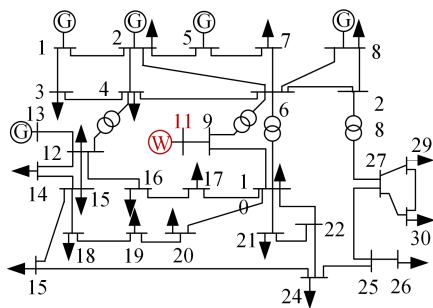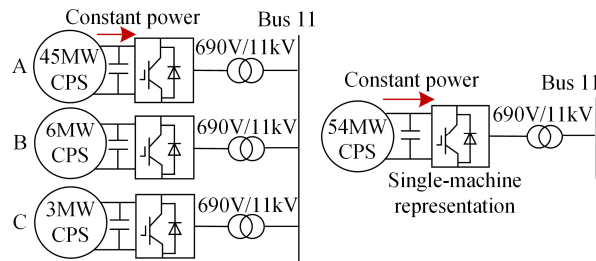
Fig. 3. IEEE 30 test system.

Fig. 4. Aggregated model of the WF. (a) Coherent equivalence model. (b) Single-machine aggregated model.

Applying the modal analysis to an *n*-CCBGs-integrated power system shown in (42), the impact of CCBGs on small-signal stability resulting from dynamic interactions can be evaluated quantitively. Obviously, if every CCBG is modeled in detail in (29), the order of the system is high. However, when CCBGs are grouped and aggregated based on the coherency identification results, the model of CCBG can be simplified and the order of the whole system can be reduced significantly, especially for those power systems integrated with large-scale CCBG plants. When coherent equivalence model is applied to the analysis of the dynamic interaction, the small-signal model of the aggregated CCBGs should be established first according to (29) using the equivalent parameters calculated by (13), (15), (17), and (19).

To summarize, the procedure of the application of coherent equivalence model in the small-signal stability analysis is:

i) establishing the coherent equivalence model of multiple inverters, which preserves the original structure of a single inverter, as stated in section II;

ii) linearizing the dynamic equations of aggregated inverters, as is shown in (29);

iii) establishing the linearized model of the whole power system by integrating the model of SGs part and CCBGs part, as is shown in (42);

iv) conducting modal analysis based on the linearized model of the whole system.

IV. CASE STUDY

A. Description of the Test System

In this section, IEEE 30 bus test system is used as an example to validate the applicability of the aggregation modeling in small-signal analysis. The configuration of the test system is shown in Fig. 3. Compared with the original 6-machine standard test system, the generator connected to bus 11 was replaced by a 54 MW PMSG-based WF in this case. The WF contains 6

TABLE I
THE RESULT OF COHERENCY IDENTIFICATION

Coherent group	Inverter number
A	1,2,3,4,5,7,8,9,11
B	6,10
C	12

TABLE II
INVERTER PARAMETERS

	S_B(MW)	L(mH)	C(F)	K_{pi}	K_{ii}	K_{pv}	K_{iv}	k_{pth}	k_{ith}
1	6	0.2	0.06	360	22.5	0.33	20	20	140
2	6	0.2	0.06	360	22.5	0.33	20	20	140
3	6	0.18	0.06	324	20.3	0.33	20	20	140
4	3	0.4	0.03	750	40	0.17	9.8	20	140
5	6	0.18	0.06	324	20.3	0.33	20	20	140
6	3	0.4	0.033	710	35	0.2	10.7	50	180
7	6	0.18	0.06	324	20.3	0.33	20	20	140
8	3	0.4	0.03	750	40	0.17	9.8	20	140
9	3	0.42	0.03	788	42	0.17	9.8	20	140
10	3	0.4	0.033	710	35	0.2	10.7	50	180
11	6	0.21	0.06	378	23.6	0.33	20	20	140
12	3	0.4	0.033	720	45	0.5	20	50	180

TABLE III
PARAMETERS OF COHERENT EQUIVALENCE MODEL

	S_B(MW)	L(mH)	C(F)	K_{pi}	K_{ii}	K_{pv}	K_{iv}	k_{pth}	k_{ith}
A	45	0.0258	0.45	46.5	2.90	2.49	149.4	20	140
B	6	0.2	0.066	355	17.5	0.4	21.4	50	180
C	3	0.4	0.033	720	45	0.5	20	50	180

TABLE IV
PARAMETERS OF SINGLE-MACHINE AGGREGATED MODEL

S_B(MW)	L(mH)	C(F)	K_{pi}	K_{ii}	K_{pv}	K_{iv}	k_{pth}	k_{ith}
54	0.2	0.055	40	2.5	3.39	190.8	27.5	150

PMSGs with 6 MW capacity each and 6 PMSGs with 3 MW capacity each. All the generators are connected to a 690 V/11 kV transformer respectively. The mechanical part and MSC of PMSG-based WTGs is represented by a constant power source (CPS), because dynamic interactions of concern actually exists between GSC and SGs [4], [5].

B. Aggregated Model of Grid-Connected Inverters

All grid-connected inverters are controlled by VOC strategy under unity power factor in the normal state, and the parameters of them are listed in Table II. In addition, all the inverters are equipped with crowbar circuit to prevent the overvoltage of the dc-link capacitor.

As stated in Section II, line currents of grid-connected inverters in dynamic process are needed for identification of coherency. To obtain the dynamic currents, the model of 12 inverters connected to an infinite bus is simulated. A three-phased fault is set at 0.1s and self-cleared at 0.2s to generate a transient of inverters. In this case, the coherency of inverters can be identified by recording the line currents during this dynamic process and calculating the maximum mean deviation between every two inverters. The result of coherency identification is obtained based on (12) and listed in Table I.

Based on the result of coherency identification, the coherent equivalence model of 12 grid-connected inverters in the WF can be established. Meanwhile, the single-machine aggregated model without consideration of coherency is established for comparison. Fig. 4 shows the schematic of the two aggregated models. The equivalent parameters of coherent equivalence model and single-machine aggregated model are calculated
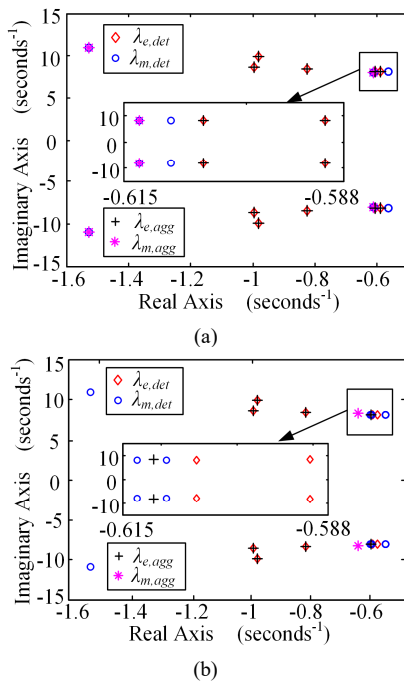
Fig. 5. Modes of the test system obtained by detailed model, coherent equivalence model and single-machine model. (a) Coherent equivalence model. (b) Single-machine aggregated model.
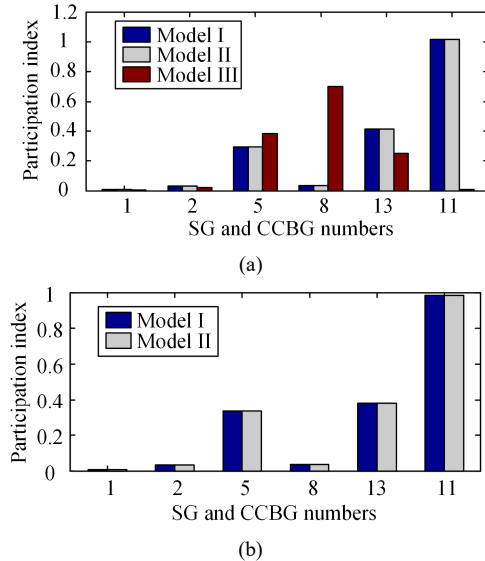

Fig. 6. Comparison of SG PI and GSC PI for mode 4 and mode 5 obtained by Model I, Model II, and Model III. (a) SG PI and GSC PI for mode 4. (b) SG PI and GSC PI for mode 5.

based on (13), (15), (17), and (19), and are listed in Table III and Table IV, respectively.

C. Analysis of Dynamic Interactions Using the Detailed and Aggregated Models

The linearized model of the WF-integrated power system using the detailed representation, the coherent equivalence representation, and the single-machine representation are built for modal analysis. These linearized models are abbreviated for Model I, Model II, and Model III, respectively, in following texts. The EOMs identified by Model I, II, and III are listed in Table V, Table VI, Table VII, respectively. Eigenvalues λ,

TABLE V
EOMs OBTAINED BY DETAILED REPRESENTATION OF VSCs

Modes	λ	f(Hz)	ζ (%)	GSC PI
1	-0.9820±9.9195i	1.5787	9.85%	0.0006
2	-0.9953±8.6131i	1.3708	11.48%	0.0002
3	-0.8260±8.4495i	1.3448	9.73%	0.0019
4	-0.5904±8.1485i	1.2969	7.23%	**1.0176**
5	-0.6053±8.1092i	1.2906	7.44%	**0.9855**

TABLE VI
EOMs OBTAINED BY COHERENT EQUIVALENCE REPRESENTATION OF VSCs

Modes	λ	f(Hz)	ζ (%)	GSC PI
1	-0.9820±9.9195i	1.5787	9.85%	0.0006
2	-0.9953±8.6131i	1.3708	11.48%	0.0002
3	-0.8260±8.4495i	1.3448	9.73%	0.0019
4	-0.5904±8.1485i	1.2969	**7.23%**	**1.0176**
5	-0.6053±8.1092i	1.2906	**7.44%**	**0.9855**

TABLE VII
EOMs OF OBTAINED BY SINGLE-MACHINE REPRESENTATION OF VSCs

Modes	λ	f(Hz)	ζ (%)	GSC PI
1	-0.9816±9.9195i	1.5787	9.85%	0.0004
2	-0.9953±8.6130i	1.3708	11.48%	0.0004
3	-0.8260±8.4482i	1.3446	9.73%	0.0090
4	-0.6110±8.1313i	1.2941	**7.49%**	**0.0131**
--	--	--	--	--

frequency f, damping ratio ζ and GSC PI corresponding to these EOMs are also listed in Table V-VII. A part of eigenvalues is shown in Fig. 5, where λ_e and λ_m are EOMs and other modes, respectively, and the subscripts *det* and *agg* indicate modes of detailed model and aggregated models, respectively.

It is important to observe from Fig. 5 and Table V-VII that mode 5 vanishes in Model III, and the damping ratio of mode 4 calculated by Model III is bigger than that calculated by Model I and II. By contrast, the result of modal analysis obtained from Model I and Model II fit well. In addition, the participation of CCBG state variables of Model III in EOMs is small, as is indicated in GSC PI. However, high participation of CCBG state variables in EOM 4 and EOM 5 can be seen in Model I and Model II. It means that the significant dynamic interaction between CCBGs and SGs can be identified when inverters are represented by the detailed model and the proposed coherent equivalence model, but this cannot be recognized when inverters are aggregated without consideration of coherency.

To analyze the participation of state variables associated with each generator in EOMs 4 and 5, SG PIs of EOM 4 and EOM 5 are calculated for all the SGs in the system. SG PIs and GSC PIs in EOM 4 and EOM 5 calculated by 3 different models are compared in Fig. 6 (a) and (b), respectively. It can be seen from Fig. 6 that the state variables of SG 5 and SG 13 participate heavily in both EOM 4 and EOM 5. This conclusion can be drawn from either the detailed model or the two aggregated models. It is clear that the dynamic interaction among CCBGs, SG 5, and SG 13 can be identified in Model I and Model II, while Model III cannot see this phenomenon. This is because single-machine representation cannot reveal the dynamic characteristics of multiple inverters when these individuals exhibit different dynamic responses under a disturbance.

Time-domain simulation is conducted by PSCAD/EMTDC using the detailed model, the coherent equivalence model and the single-machine aggregated model of GSCs to verify the results of modal analysis. A 0.1 p.u. rise of output active power
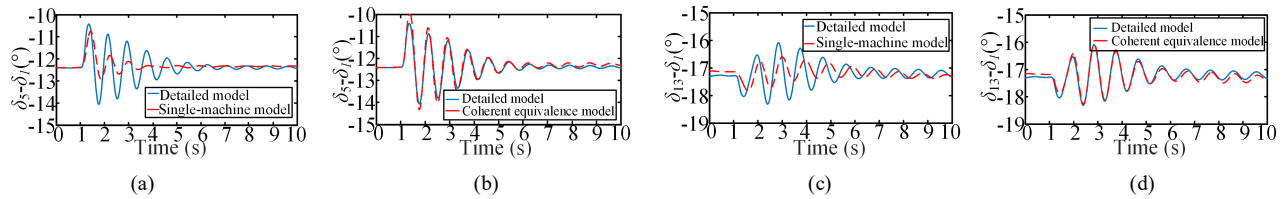
Fig. 7. Comparison of the rotor angle simulated by aggregated models and the detailed model. (a) SG 5, the single-machine model. (b) SG 5, the coherent equivalence model. (c) SG 13, the single-machine model. (d) SG 13, the coherent equivalence model.
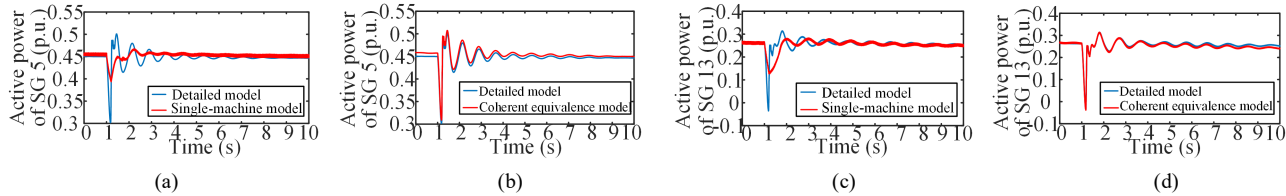

Fig. 8. Comparison of the active power simulated by aggregated models and the detailed model. (a) SG 5, the single-machine model. (b) SG 5, the coherent equivalence model. (c) SG 13, the single-machine. (d) SG 13, the coherent equivalence model.

of CCBGs which last for 0.2 s is set as a small disturbance to excite the dynamics of the power system. As the states of SG 5 and SG 13 are the main states that participate in EOM 4 and EOM 5, the electromechanical characteristics (rotor angle and active power) of them are detected and compared, as is shown in Fig. 7 and Fig. 8.

The results obtained by the detailed model (see Fig. 7 and Fig. 8) substantiate that the pulse change in the active power output of CCBGs can excite the oscillation of rotor angle of SG 5 and SG 13, which participate largely in EOM 4 and EOM 5. This time-domain result verifies the dynamic interactions between CCBGs and SGs. Meanwhile, it can be seen from Fig. 7 and Fig. 8 that the dynamic responses obtained from the detailed model and the coherent equivalence model fit well. By contrast, the rotor angle and power curves obtained from the single-machine aggregated model did not oscillate as the pulse change occurred in the active power output of CCBGs. That is to say, the dynamic interaction of the system cannot be observed when CCBGs are modeled by a single-machine aggregated model. Time-domain simulation results agree with the results of modal analysis and also demonstrate the advantage of the coherent equivalence model in the application of the small-signal analysis of CCBGs-integrated power systems, especially the dynamic interaction between CCBGs and SGs.

V. CONCLUSIONS

In this paper, the aggregated model of multiple inverters has been established by the proposed Hamilton's-action-based coherent equivalence method, and the applicability of the aggregated model in the small-signal stability analysis of CCBGs-integrated power systems is validated.

The Hamilton's-action-based coherency criterion and its equivalent current-based criterion are derived based on the Hamilton modeling of inverters. The coherent inverters identified by the proposed criterion can be aggregated after calculation of equivalent parameters.

To apply the coherent equivalence modeling of inverters to small-signal stability analysis, the linearized model of the aggregated representation of multiple inverters should be established and integrated with the small-signal model of SGs. Modal analysis based on the linearized model of the whole system can effectively identify the impact of CCBGs on the small-signal stability of power systems resulting from the dynamic interaction.

A comparative analysis was presented between the proposed coherent equivalence model and the traditional single-machine aggregated model. Modal analysis and simulation results obtained from the detailed model and the single-machine aggregated model showed differences in EOMs and rotor angle responses. By contrast, the coherent equivalence model not only simplified the computational complexity, but also preserved the characteristics of EOMs and the dynamic interaction between CCBGs and SGs. Frequency and time domain analysis both suggested the advantage of the coherent equivalence in the practice of small-signal stability analysis. In future work, the proposed aggregation method will be further developed by taking the dynamics of mechanical parts into consideration to meet the needs of more dynamic analysis applications.

APPENDIX A

From the definition of $\hat{S}$ shown in (3), we have:

$$\delta \hat{S} = \delta S - \delta U = \delta S + \delta \int (\sum_{j=1}^{N} \int_{\gamma} Q_j dq_j) dt \qquad (A.1)$$

As the order of the integral operation and the variational operation can be exchanged, (A.1) can be transformed into:

$$\delta \hat{S} = \delta S + \int [\sum_{j=1}^{N} \delta (\int Q_j \dot{q}_j dt)] dt \qquad (A.2)$$

Meanwhile, in (A.2), we have:

$$\delta (\int Q_j \dot{q}_j dt) = \int \delta (Q_j \dot{q}_j) dt = \int (Q_j \delta \dot{q}_j + \dot{q}_j \delta Q_j) dt \quad (A.3)$$

The order of the differential operation and the variational operation can be exchanged as well, so (A.3) is rewritten as:

$$\delta (\int Q_j \dot{q}_j dt) = Q_j \delta q_j + \int (\dot{q}_j \delta Q_j - \dot{Q}_j \delta q_j) dt \qquad (A.4)$$

Physically, the nonconservative forces Q_j are related with q_j and $\dot{q}_j$ simultaneously. By using the phase trajectory and subdividing the time domain, $\dot{q}_j$ can be substituted by q_j, and then Q_j can be written as the function of q_j. Thus, we have:

$$\delta Q_j = \frac{dQ_j}{dq_j} \delta q_j \qquad (A.5)$$

Substitute (A.5) into (A.4):

$$\delta (\int Q_j \dot{q}_j dt) = Q_j \delta q_j \qquad (A.6)$$

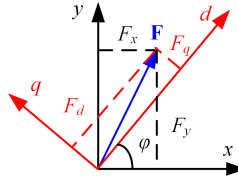Substitute (A.6) into (A.2), and then combines (A.2) and (1):

Fig. B1.   Transformation of *dq* components of variables to *xy* axis.

$$\delta \hat{S} = \delta S + \int \sum_{j=1}^{N} Q_j \delta q_j \, dt = 0 \qquad (A.7)$$

So far, the equivalence between (1) and (4) has been proved.

APPENDIX B

When d axis leads x axis by φ, as is shown in Fig. B1, the transformation of xy components into dq axis is obtained by

$$\begin{bmatrix} F_x \\ F_y \end{bmatrix} = \begin{bmatrix} \cos\varphi & -\sin\varphi \\ \sin\varphi & \cos\varphi \end{bmatrix} \begin{bmatrix} F_d \\ F_q \end{bmatrix} \qquad (B.1)$$

As d-axis of inverters is set oriented to the bus voltage vector, the angle between the d- and x-axis equals to the CCBGs-connected bus voltage angle θ. Substitute θ into (B.1) and linearize the xy-dq transformation equation:

$$\Delta \mathbf{I}_{ci,xy} = \mathbf{T}_{v0} \Delta \mathbf{I}_{ci,dq} + \mathbf{B}_{vIi} \Delta\theta \qquad (B.2)$$

where the subscript i indicates variables of the ith CCBG, and

$$\mathbf{T}_{v0} = \begin{bmatrix} \cos\theta_0 & -\sin\theta_0 \\ \sin\theta_0 & \cos\theta_0 \end{bmatrix} \qquad (B.3)$$

$$\mathbf{B}_{vIi} = \begin{bmatrix} -\sin\theta_0 I_{ci,d0} - \cos\theta_0 I_{ci,q0} \\ \cos\theta_0 I_{ci,d0} - \sin\theta_0 I_{ci,q0} \end{bmatrix}. \qquad (B.4)$$

In (B.3) and (B.4), θ_0 is the initial value of θ.

As q-axis is oriented to the inner potential $\mathbf{E}_q$, the angle between q- and x-axis equals to the angle of $\mathbf{E}_q$, which is represented by δ. Thus, the angle between d- and x-axis is δ-$\pi/2$. Substitute δ-$\pi/2$ for the φ in (B.1) and linearize the xy-dq transformation equation:

$$\Delta \mathbf{I}_{gj,xy} = \mathbf{T}_{g0j} \Delta \mathbf{I}_{gj,dq} + \mathbf{B}_{gIj} \Delta\delta_j \qquad (B.5)$$

where the subscript j indicates variables of the jth SG, and

$$\mathbf{T}_{g0j} = \begin{bmatrix} \sin\delta_{j0} & \cos\delta_{j0} \\ -\cos\delta_{j0} & \sin\delta_{j0} \end{bmatrix} \qquad (B.6)$$

$$\mathbf{B}_{gIj} = \begin{bmatrix} \cos\delta_{j0} I_{gj,d0} - \sin\delta_{j0} I_{gj,q0} \\ \sin\delta_{j0} I_{gj,d0} + \cos\delta_{j0} I_{gj,q0} \end{bmatrix}. \qquad (B.7)$$

In (B.6) and (B.7), δ_0 is the initial value of δ. In fact, the δ_j is the rotor angle of the jth SG, so that it is an element of $\mathbf{X}_{gen}$. Thus, the coefficient matrices $\mathbf{T}_{g0}$ and $\mathbf{B}_{gI}$ in (34) can be obtained by $\mathbf{T}_{g0j}$ and $\mathbf{B}_{gIj}$ shown in (B.6) and (B.7).

REFERENCES

[1] E. Vittal, M. O'Malley and A. Keane, "Rotor angle stability with high penetrations of wind generation," *IEEE Trans. Power Syst.*, vol. 27, no. 1, pp. 353-362, Feb. 2012.

[2] G. Tsourakis, B. M. Nomikos and C. D. Vournas, "Contribution of doubly fed wind generators to oscillation damping," *IEEE Trans. Energy Convers.*, vol. 24, no. 3, pp. 783-791, Sept. 2009.

[3] T. Knuppel, J. N. Nielsen, K. H. Jensen, A. Dixon and J. Ostergaard, "Small-signal stability of wind power system with full-load converter interfaced wind turbines," *IET Renew. Power Gener.*, vol. 6, no. 2, pp. 79-91, March 2012.

[4] J. Quintero, V. Vittal, G. T. Heydt and H. Zhang, "The impact of increased penetration of converter control-based generators on power System modes of oscillation," *IEEE Trans. Power Syst.*, vol. 29, no. 5, pp. 2248-2256, Sept. 2014.

[5] W. Du, J. Bi, J. Cao and H. F. Wang, "Method to examine the impact of grid connection of the DFIGs on power system electromechanical oscillation modes," *IEEE Trans. Power Syst.*, vol. 31, no. 5, pp. 3775-3784, Sept. 2016.

[6] D. Gautam and V. Vittal, "Impact of increased penetration of DFIG-Based wind farm generators on transient and small signal stability of power systems," *IEEE Trans. Power Syst.*, vol. 24, no. 3, pp. 1426–1434, Aug. 2009.

[7] A. Mendonca and J. A. P. Lopes, "Impact of large scale wind power integration on small signal stability," *2005 International Conference on Future Power Syst.*, Amsterdam, 2005, pp. 1-5.

[8] W. Du, X. Chen and H. F. Wang, "Power system electromechanical oscillation modes as affected by dynamic interactions from grid-connected PMSGs for wind power generation," *IEEE Trans. Sustain. Energy*, vol. 8, no. 3, pp. 1301-1312, July 2017.

[9] T. Knuppel, J. N. Nielsen, K. H. Jensen, A. Dixon and J. Ostergaard, "Power oscillation damping capabilities of wind power plant with full converter wind turbines considering its distributed and modular characteristics," *IET Renew. Power Gener.*, vol. 7, no. 5, pp. 431-442, Sept. 2013.

[10] T. Knuppel, J. N. Nielsen, K. H. Jensen, A. Dixon and J. Ostergaard, "Small-signal stability of wind power system with full-load converter interfaced wind turbines," *IET Renewable Power Gener.*, vol. 6, no. 2, pp. 79-91, March 2012.

[11] N. Ding, Z. X. Lu, Y. Qiao, and Y. Min, "Simplified models of largescale wind and their applications for small-signal stability," *Journal of Modern Power Syst. and Clean Energy*, vol. 1, no.1, pp. 58–64, Jun. 2013.

[12] J. Brochu, C. Larose and R. Gagnon, "Validation of single- and multiple-machine equivalents for modeling wind power plants," *IEEE Trans. Energy Convers.*, vol. 26, no. 2, pp. 532-541, June 2011.

[13] V. Akhmatov and H. Knudsen, "An aggregate model of a grid-connected, large-scale, offshore wind farm for power stability investigations: Importance of windmill mechanical system," *Int. J. Elect. Power Energy Syst.*, vol. 24, no. 9, pp. 709–717, Nov. 2002.

[14] E. Muljadi and C. P. Butterfield, "Dynamic simulation of a wind farm with variable-speed wind turbines," *Trans. Amer. Soc. Mech. Eng.*, vol. 125, no. 4, pp. 410–417, Nov. 2003.

[15] M. Ali, I. S. Ilie, J. V. Milanovic and G. Chicco, "Wind farm model aggregation using probabilistic clustering," *IEEE Trans. Power Syst.*, vol. 28, no. 1, pp. 309-316, Feb. 2013.

[16] V. Purba, S. V. Dhople, and S. Jafarpour, F. Bullo, etc. "Reduced-order structure-preserving model for parallel-connected three-phase grid-tied inverters," *2017 COMPEL*, Stanford, CA, 2017, pp. 1-7.

[17] V. Purba, S. V. Dhople, S. Jafarpour, F. Bullo and B. B. Johnson, "Network-cognizant model reduction of grid-tied three-phase inverters," *2017 55th Annual Allerton Conference on Communication, Control, and Computing (Allerton)*, Monticello, IL, 2017, pp. 157-164.

[18] X. Du, Y. Zhang, Q. Li, Y. Xiong, X. Yu and X. Zhang, "New theory of extended coherency for power system based on method of coherency in differential geometry," in *APPEEC, 2011 Asia-Pacific*, Wuhan, 2011, pp. 1-6.

[19] C. Li, J. Xu and C. Zhao, "A coherency-based equivalence method for MMC inverters using virtual synchronous generator control," *IEEE Trans. Power Del.*, vol. 31, no. 3, pp. 1369-1378, June 2016.

[20] G. Joos and I. M. Freeman, *Theoretical Physics,* Hafner Publishing Company, New York, 1950.

[21] X. Zha, S. Liao, M. Huang, Z. Yang and J. Sun, "Dynamic aggregation modeling of grid-connected inverters using Hamilton's-action-based coherent equivalence," *IEEE Trans. Indus. Electron.*, early access.

[22] P. K. Sahu, P. Shaw and S. Maity, "Modeling and control of grid-connected DC/AC converters for single-phase micro-inverter application," in *INDICO*, New Delhi, 2015, pp. 1-6.

[23] A. J. Germond and R. Podmore, "Dynamic aggregation of generating unit models," *IEEE Trans. Power App. Syst.*, vol.PAS-97, no.4, pp.1060-1069, July 1978.

[24] J. Conroy and R. Watson, "Aggregate modelling of wind farms containing full-converter wind turbine generators with permanent magnet synchronous machines: transient stability studies," *IET Renew. Power Gener.*, vol. 3, no. 1, pp. 39-52, March 2009.

[25] S. Hansen, M. Malinowski, F. Blaabjerg and M. P. Kazmierkowski, "Sensorless control strategies for PWM rectifier," in *Proc. of APEC 2000 Conference*, New Orleans, LA, 2000, pp. 832-838.

Shuhan Liao (S'18) was born in Xiangtan, Hunan Province, China, in 1993. She received B.Eng. Degree in electrical engineering from Wuhan University, Wuhan, China, in 2015, where she is currently working toward the Ph.D. degree.

Since Oct. 2018, she has been a guest Ph.D. student with the Department of Energy Technology, Aalborg University, Aalborg, Denmark. Her main research interests include the modeling and dynamic analysis of renewable energy generation systems.

Xiaoming Zha (M'02) was born in Huaining, Anhui Province, China, in 1967. He received B.S., M.S., and Ph.D. degrees in electrical engineering from Wuhan University, Wuhan, China, in 1989, 1992, and 2001, respectively.

He was a Postdoctoral Fellow at the University of Alberta, Canada from 2001 to 2003. He has been a Faculty Member of Wuhan University since 1992, and became a Professor in 2003. He is currently the Deputy Dean in the school of electrical engineering, Wuhan University, Wuhan, China. His research interests include power electronic converter, the application of power electronics in smart grid and renewable energy generation, the analysis and control of microgrid, the analysis and control of power quality, and frequency control of high-voltage high-power electric motors.

Xianzhe Li was born in Yongzhou, Hunan Province, China, in 1996. He received the B.Eng. in electrical engineering from Wuhan University, Wuhan, China, in 2018, where he is currently working toward the M.Eng. degree.

His main research interests include the modeling and low frequency oscillation analysis of renewable energy generation systems.

Meng Huang (S'11–M'13) received the B.Eng. and M.Eng. degrees from Huazhong University of Science and Technology, Wuhan, China, in 2006 and 2008, respectively, and the Ph.D. degree from the Hong Kong Polytechnic University, Hong Kong, in 2013.

He is currently an Associate Professor of the School of Electrical Engineering, Wuhan University, Wuhan, China. His research interests include nonlinear analysis of power converters and power electronics reliability.

Jianjun Sun (M'13) was born in 1975. He received the B.Eng., M.Eng., and Ph.D. degrees in electrical engineering from Wuhan University, Wuhan, China, in 1997, 2000, and 2007, respectively.

He is currently with the School of Electrical Engineering, Wuhan University as an Associate Professor and the Deputy Director of the Motor and Power Electronics Center. His current research interests include modeling and analysis of power-electronic system and microgrid.

Jing Pan received the B.Eng. degrees from Southeast University, Nanjing, China, in 1991 and the MBA degree from the Hefei University of Technology, Hefei, China in 2014.

She is a senior engineer at State Grid Anhui Electric Power Co., Ltd., Hefei, China. Her main research interests include renewable energy generation and energy storage technology.

Josep M. Guerrero (S'01–M'04–SM'08–F'15) received the B.S. degree in telecommunications engineering, the M.S. degree in electronics engineering, and the Ph.D. degree in power electronics from the Technical University of Catalonia, Barcelona, Spain, in 1997, 2000, and 2003, respectively.

Since 2011, he has been a Full Professor with the Department of Energy Technology, Aalborg University, Aalborg, Denmark, where he is responsible for the Microgrid Research Program (www.microgrids.et.aau.dk). His research interests include different microgrid aspects, including power electronics, distributed energy-storage systems, hierarchical and cooperative control, energy management systems, smart metering, and the Internet of Things for ac–dc microgrid clusters and islanded minigrids; recently specially focused on maritime microgrids for electrical ships, vessels, ferries, and seaports.

Dr. Guerrero is an Associate Editor for the *IEEE TRANSACTIONS ON POWER ELECTRONICS*, the *IEEE TRANSACTIONS ON INDUSTRIAL ELECTRONICS*, and the *IEEE INDUSTRIAL ELECTRONICS MAGAZINE*, and an Editor for the *IEEE TRANSACTIONS ON SMART GRID*.